Fundamental measure theory for the inhomogeneous hard-sphere system based on Santos' consistent free energy

Hendrik Hansen-Goos,[1,*] Mostafa Mortazavifar,[2] Martin Oettel,[2] and Roland Roth[1]
[1]*Institute for Theoretical Physics, University of Tübingen, Auf der Morgenstelle 14, 72076 Tübingen, Germany*
[2]*Institute for Applied Physics, University of Tübingen, Auf der Morgenstelle 10, 72076 Tübingen, Germany*
(Received 23 March 2015; published 14 May 2015)

Based on Santos' general solution for the scaled-particle differential equation [Phys. Rev. E **86**, 040102(R) (2012)], we construct a free-energy functional for the hard-sphere system. The functional is obtained by a suitable generalization and extension of the set of scaled-particle variables using the weighted densities from Rosenfeld's fundamental measure theory for the hard-sphere mixture [Phys. Rev. Lett. **63**, 980 (1989)]. While our general result applies to the hard-sphere mixture, we specify remaining degrees of freedom by requiring the functional to comply with known properties of the pure hard-sphere system. Both for mixtures and pure systems, the functional can be systematically extended following the lines of our derivation. We test the resulting functionals regarding their behavior upon dimensional reduction of the fluid as well as their ability to accurately describe the hard-sphere crystal and the liquid-solid transition.

DOI: 10.1103/PhysRevE.91.052121 PACS number(s): 05.70.Ce, 61.20.Gy, 65.20.Jk

I. INTRODUCTION

The hard-sphere system is a simple yet very important model system in classical statistical physics. Both colloidal [1] and molecular systems [2] can give rise to interactions that are well described by the hard-sphere model where particles either do not interact, as long as their hard cores do not overlap, or experience an infinite repulsion, in the case where an overlap is attempted. For general interactions the hard-sphere model provides an important reference system to which more elaborate, generally attractive, forces can be added in perturbative treatments [3]. Even the pure hard-sphere system exhibits nontrivial phase behavior in the form of a first-order liquid-to-crystal transition [4].

One great benefit of the hard-sphere model is that very accurate theoretical descriptions of both the homogeneous and inhomogeneous fluid, and of the crystal phase are available through a variety of methods [5], including perturbative expansions, integral equation theory, and density functional theory (DFT). The Percus-Yevick closure of integral equations [6,7] allows for an analytical solution yielding approximations to the direct correlation function, the structure factor, and the equation of state of the homogeneous fluid, which are widely used as a reference. The extension of the integral equation method to inhomogeneous fluids gives accurate results (see, e.g., Refs. [8–10]) but the solutions become cumbersome from a numerical point of view. These numerical difficulties are part of the reason why the crystal phase (being an extreme realization of an inhomogeneous liquid) is largely unexplored via integral equations; see, however, Ref. [11].

In contrast to integral equations, classical DFT [12,13], which is based on a variational principle, provides a particularly powerful framework for the treatment of fluid and crystal phases in arbitrary external potentials and shall be the focus of the present study. Classical DFT is also the starting point for the derivation of the phase field crystal (PFC) model, a generic coarse-grained model of the crystal phase [14]. In this context, accurate DFT descriptions of the hard-sphere crystal and solid-liquid interfaces serve as benchmarks for the PFC modeling [15].

DFT of classical fluids in general [16], and of the hard-sphere system in particular, has been studied since the late 1970s, but only since 1989, when Rosenfeld introduced the fundamental measure theory (FMT) of hard-sphere fluid mixtures [17], has a theory been available that has led to DFT descriptions of both the fluid and crystal, which exhibit excellent agreement with numerical simulations and experimental findings. Rosenfeld's work has inspired a lot of studies both on applications of DFT to a large variety of phenomena, and on ways to further improve FMT functionals. These improvements of the original FMT can be divided into two sectors. One body of work is devoted to improving the equation of state (EOS) that is underlying the FMT, while the other focuses on regularizing spurious divergences that are inherent to Rosenfeld's original FMT.

Basically, two routes have been employed in previous work in order to regularize the spurious divergences of the original FMT, which appear when strongly peaked density distributions are studied. The first empirical modifications were based upon the original set of Rosenfeld's scalar and vectorial weighted densities [18], while later work introduced an additional tensorial weighted density [19,20]. Both approaches allow for a successful description of crystals within FMT.

Regarding the implementation of more accurate EOSs it should be noted that the original FMT obeys the Percus-Yevick EOS, which is known to be inaccurate for large packing fractions of the fluid. In contrast, the accurate Carnahan-Starling EOS [21] is used as an input for the so-called White Bear versions of FMT [22–24]. In the original White Bear FMT, the use of the CS EOS leads to an inconsistency with an exact relation from scaled-particle theory [22]. In the White Bear Mark II (WBII) version of FMT, this inconsistency is removed for the pure hard-sphere fluid; however, it is still found for the hard-sphere mixture [24].

Recently, Santos has shown how the inconsistency arising from using the CS EOS within FMT can be eliminated, at

*hendrik.hansen-goos@uni-tuebingen.de

least for a homogeneous bulk system, even for mixtures [25]. A simple extension toward inhomogeneous systems has been proposed by Santos [25]; however, the approach has been shown to lead to unphysical behavior [26]. In particular, the direct correlation function of the hard-sphere fluid as derived from the Santos FMT has a spurious divergence for $r \to 0$.

In the present paper we introduce an extension of Santos free energy to inhomogeneous systems, which generates a well-behaved direct correlation function, i.e., the problem reported by Lutsko [26] is cured. When applied to the pure hard-sphere fluid, the results of our new functional are of an accuracy similar to those from the WBII version of FMT. For instance, the direct correlation function derived from our new FMT is always within 1% of the WBII result for all fluid-packing fractions.

Our present FMT, which employs the original set of Rosenfeld's scalar and vectorial-weighted densities, is constructed such that it can successfully describe the hard-sphere crystal. Currently it is unclear how a tensorial-weighted density would be incorporated into the framework of Santos' free energy. When the use of the tensorial-weighted density is desired, the modified WBII version [13,24,27] still appears to be the best choice. However, the use of only scalar and vectorial-weighted densities reduces the complexity of the functional, which is important, especially for time-consuming 3D computations or if results using analytical methods are required.

The paper is organized as follows. In Sec. II we review Santos' consistent free energy for the hard-sphere mixture in bulk and we present the general formulation of our free-energy functional for the inhomogeneous hard-sphere mixture. In Sec. III we focus on the case of a pure hard-sphere system, i.e., a system of equally sized hard spheres, in order to specify remaining degrees of freedom. We consider both an approach that is based on dimensional reduction as well as the introduction of an empirical parameter. We demonstrate that, in additional to being very accurate for the hard-sphere fluid, the new functional is able to correctly describe the hard-sphere crystal. Finally, in Sec. IV we summarize our findings and present our conclusions.

II. GENERAL FORMULATION OF THE FREE ENERGY FUNCTIONAL

A. Santos' free energy for hard-sphere mixtures in bulk

Santos' free energy for the ν-component hard-sphere mixture in bulk is obtained as a function of the well-established scaled-particle variables

$$\xi_0 = \sum_{i=1}^{\nu} \rho_i, \quad \xi_1 = \sum_{i=1}^{\nu} R_i \rho_i, \quad \xi_2 = \sum_{i=1}^{\nu} 4\pi R_i^2 \rho_i, \quad \text{and}$$
$$\xi_3 = \sum_{i=1}^{\nu} \frac{4\pi}{3} R_i^3 \rho_i, \tag{1}$$

where R_i and ρ_i are the radius and number density of species i, respectively.

In scaled-particle theory (SPT) the simplifying assumption is made that the free-energy density Φ of the system is a function only of the scaled-particle variables $\xi_0, \ldots, \xi_3$. Using an exact relation regarding the energy required to reversibly introduce an infinitely large sphere into the system, the following SPT differential equation can be obtained [17]:

$$\frac{\partial \Phi}{\partial \xi_3} = \xi_0 - \Phi + \sum_{j=0}^{3} \frac{\partial \Phi}{\partial \xi_j} \xi_j. \tag{2}$$

A solution for Eq. (2) can be obtained based on dimensional analysis. It can be shown that the only monomials which have the dimension of Φ are ξ_0, $\xi_1\xi_2$, and ξ_2^3. Using the ansatz that $\Phi = f(\xi_3)\xi_0 + g(\xi_3)\xi_1\xi_2 + h(\xi_3)\xi_2^3$, where f, g, and h are arbitrary functions of the dimensionless variable ξ_3, we find the solution

$$\Phi_{\mathrm{PY}} = -\xi_0 \ln(1-\xi_3) + \frac{\xi_1\xi_2}{1-\xi_3} + \frac{\xi_2^3}{24\pi(1-\xi_3)^2}, \tag{3}$$

where integration constants have been chosen such that for the dilute system the correct virial coefficients are recovered. Interestingly, Φ_{PY} is identical to the free energy obtained for the hard-sphere mixture upon solving the Ornstein-Zernike equation with the Percus-Yevick closure and using the compressibility route to compute the pressure, hence the index PY.

Only recently, Santos derived the general solution to Eq. (2), which can be written as [25]

$$\Phi_{\mathrm{Santos}} = -\xi_0 \ln(1-\xi_3) + \frac{\xi_1\xi_2}{1-\xi_3} + \frac{\xi_2^3}{24\pi(1-\xi_3)^2} f_0(y_\xi), \tag{4}$$

where $y_\xi = \frac{\xi_2^2}{12\pi\xi_1(1-\xi_3)}$ and f_0 is an arbitrary function of y_ξ. The original scaled-particle expression Eq. (3) is recovered for

$$f_0^{\mathrm{PY}}(y) = 1. \tag{5}$$

One obvious advantage of Eq. (4) over Eq. (3) is that the function f_0 can be chosen such that an arbitrary EOS is recovered from Φ_{Santos} in the limit of a pure fluid. In particular, the very accurate Carnahan-Starling EOS leads to

$$f_0^{\mathrm{CS}}(y) = \frac{2}{3y} + \frac{2}{3} - \frac{2\ln(1+y)}{3y^2} = 1 - \frac{2y}{9} + \frac{y^2}{6} + \mathcal{O}(y^3). \tag{6}$$

B. Functional for the inhomogeneous hard-sphere mixture

In order to make contact with FMT for the inhomogeneous hard sphere system, we introduce the weighted densities $n_0, \ldots, n_3$, $\mathbf{n}_1$, and $\mathbf{n}_2$, which are obtained from a convolution,

$$n_j(\mathbf{r}) = \sum_{i=1}^{\nu} \int d\mathbf{r}' \rho_i(\mathbf{r}') \omega_i^{(j)}(\mathbf{r} - \mathbf{r}'), \tag{7}$$

of the density profiles $\rho_i(\mathbf{r})$ of the individual components of the fluid mixtures with the weight functions

$$\omega_i^{(0)}(\mathbf{r}) = \frac{1}{4\pi R_i^2}\delta(R_i - r), \quad \omega_i^{(1)}(\mathbf{r}) = \frac{1}{4\pi R_i}\delta(R_i - r),$$
$$\omega_i^{(2)}(\mathbf{r}) = \delta(R_i - r),$$
$$\omega_i^{(3)}(\mathbf{r}) = \Theta(R_i - r), \quad \boldsymbol{\omega}_i^{(1)}(\mathbf{r}) = \frac{\hat{\mathbf{r}}}{4\pi R_i}\delta(R_i - r),$$
$$\boldsymbol{\omega}_i^{(2)}(\mathbf{r}) = \hat{\mathbf{r}}\delta(R_i - r), \tag{8}$$

where $r = |\mathbf{r}|$ and $\hat{\mathbf{r}} = \mathbf{r}/r$. In the homogeneous fluid, the scalar weighted densities $n_0, \ldots, n_3$ reduce to $\xi_0, \ldots, \xi_3$ and the vectorial weighted densities $\mathbf{n}_1$ and $\mathbf{n}_2$ vanish.

The weighted densities $n_0, \ldots, n_3$, $\mathbf{n}_1$, and $\mathbf{n}_2$ were first introduced by Rosenfeld who constructed the first FMT free energy density

$$\Phi_{\mathrm{RF}} = -n_0 \ln(1-n_3) + \frac{n_1 n_2 - \mathbf{n}_1 \cdot \mathbf{n}_2}{1-n_3} + \frac{n_2^3 - 3n_2(\mathbf{n}_2 \cdot \mathbf{n}_2)}{24\pi(1-n_3)^2}, \tag{9}$$

which reduces to Eq. (3) for a bulk mixture. The grand potential functional that results from an FMT excess free-energy density $\Phi = \Phi(\{n_j\})$ is given by

$$\Omega[\{\rho_i\}] = \mathcal{F}_{\mathrm{id}}[\{\rho_i\}] + \beta^{-1} \int \Phi(\{n_j\})\, d\mathbf{r} + \sum_{i=1}^{\nu} \int \rho_i(\mathbf{r})[V_i(\mathbf{r}) - \mu_i] d\mathbf{r}, \tag{10}$$

where $\mathcal{F}_{\mathrm{id}}$ is the free-energy functional of the ideal gas, $\beta^{-1} = k_B T$, μ_i denotes the chemical potential of species i, and V_i is the external potential acting on species i, which gives rise to the inhomogeneity [12]. The functional Ω with the free energy density $\Phi = \Phi_{\mathrm{RF}}$ has been shown to describe many aspects of nonuniform hard-sphere fluids very well. In particular, Φ_{RF} becomes exact in the dilute limit. The underlying direct correlation function is identical to that obtained within integral equations using the PY closure.

In order to generalize Φ_{Santos} from Eq. (4) to the inhomogeneous fluid, we define two additional weighted densities

$$\bar{n}_1 = n_1 - (\mathbf{n}_1 \cdot \mathbf{n}_2)/n_2 \quad \text{and} \quad \bar{n}_2 = n_2 - (\mathbf{n}_2 \cdot \mathbf{n}_2)/n_2. \tag{11}$$

Using the set $\{n_0, n_1, \bar{n}_1, n_2, \bar{n}_2, n_3\}$ we suggest the general (gen) form

$$\Phi_{\mathrm{gen}} = -n_0 \ln(1-n_3) + \frac{\bar{n}_1 n_2}{1-n_3} + \frac{\bar{n}_2^2 n_2}{24\pi(1-n_3)^2} \times F\left[\frac{\bar{n}_2^2}{12\pi \bar{n}_1 (1-n_3)}, \frac{\bar{n}_1}{n_1}, \frac{\bar{n}_2}{n_2}\right], \tag{12}$$

where F is a function of the three dimensionless arguments. We require F to remain finite in the low density limit, i.e., as the first argument of F vanishes. The form is motivated by the fact that Φ_{gen} is the most general formal solution of the scaled-particle differential equation [Eq. (2)] (where now the sum is over $\{n_0, n_1, \bar{n}_1, n_2, \bar{n}_2, n_3\}$). The requirement on F not only insures that Φ_{gen} is exact for the dilute system. It also yields the exact free energy in the strict 0D limit (see Appendix A).

III. FUNCTIONALS FOR THE PURE HARD-SPHERE SYSTEM

Except for the value at low density, i.e., when the first argument vanishes, the function F in Eq. (12) is so far unconstrained. In order to make the task of constructing a useful functional more manageable, we limit ourselves to a pure hard-sphere system in the following. Denoting the radius of the spheres by R, it follows from Eqs. (8) and (11) that $n_0 = n_2/(4\pi R^2)$, $n_1 = n_2/(4\pi R)$, and $\bar{n}_1 = \bar{n}_2/(4\pi R)$. Therefore, the complexity of the problem is significantly reduced and Φ_{gen} can be written as

$$\Phi_m = \frac{-n_2 \ln(1-n_3)}{4\pi R^2} + \frac{\bar{n}_2 n_2}{4\pi R(1-n_3)} + \frac{\bar{n}_2^2 n_2}{24\pi(1-n_3)^2} F_m\left[\frac{R\bar{n}_2}{3(1-n_3)}, \frac{\bar{n}_2}{n_2}\right]. \tag{13}$$

In order to determine a function F_m which is useful for practical applications we have expanded F from Eq. (12) in the second argument about the homogeneous limit in which $\frac{\bar{n}_2}{n_2} = 1$. Hence, we have replaced F by

$$F_m(y,x) = f_0(y) - \sum_{k=1}^{m} f_k(y)(1-x)^k, \tag{14}$$

where we denote $y = \frac{R\bar{n}_2}{3(1-n_3)}$ and $x = \frac{\bar{n}_2}{n_2}$. It is important to note that the choice of y as the argument of the coefficients in the expansion is somewhat arbitrary. Given that F is a general function of both y and x, infinitely many other combinations could be used, for instance y/x. Our reason for choosing y is that it is well-behaved in the 0D limit in which $y \to 0$ while y/x diverges (see Appendix A).

In order to determine the coefficient functions f_k, we turn to properties that we desire the functional Φ_m to possess. First, we impose an EOS for the bulk fluid. By construction, in the homogeneous fluid F_m reduces to $f_0(y)$ as in the bulk fluid we have $x \equiv 1$. Hence, we can identify $f_0(y)$ with the function introduced in Eq. (4). In particular, for the PY EOS we employ Eq. (5) while imposing the accurate CS EOS leads to f_0 from Eq. (6).

It can be shown that the direct correlation function (DCF)

$$c(r = |\mathbf{r} - \mathbf{r}'|) = -\beta \frac{\delta^2 \mathcal{F}[\rho]}{\delta\rho(\mathbf{r})\delta\rho(\mathbf{r}')}, \tag{15}$$

with $\mathcal{F} = \beta^{-1} \int \Phi_m d\mathbf{r}$ does not depend on the functions f_k for $k \geqslant 2$. Therefore, it appears to be reasonable to use the remaining degree of freedom (i.e., f_1) in order to fix the spurious divergence of the DCF for $r \to 0$, which has been a problem of a previous formulation of Φ_{Santos} for the inhomogeneous fluid [25,26]. It turns out that requiring the DCF to be finite as $r \to 0$ leads to the condition that

$$f_1(y) = f_0(y) + 2y f_0'(y) + \tfrac{1}{2} y^2 f_0''(y). \tag{16}$$

Depending on the underlying EOS the explicit results read

$$f_1^{\mathrm{PY}}(y) = 1, \tag{17}$$

$$f_1^{\mathrm{CS}}(y) = \frac{1 + \frac{4}{3}y + \frac{2}{3}y^2}{(1+y)^2} = 1 - \frac{2y}{3} + y^2 + \mathcal{O}(y^3). \tag{18}$$

Introducing the packing fraction $\eta = \frac{4\pi R^3}{3}\rho$, the resulting expressions for the DCF read

$$c_{\mathrm{PY}}(r) = -\frac{(1+2\eta)^2}{(1-\eta)^4} + \frac{3\eta(2+\eta)^2}{2(1-\eta)^4}\frac{r}{\sigma} - \frac{\eta(1+2\eta)^2}{2(1-\eta)^4}\left(\frac{r}{\sigma}\right)^3, \tag{19}$$

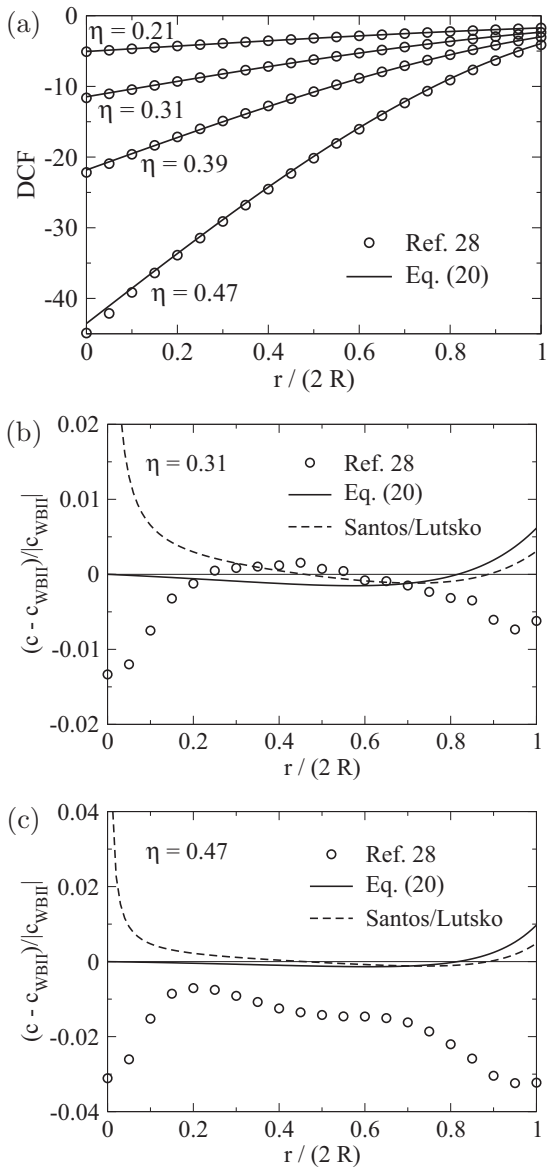

FIG. 1. Results for the direct correlation function $c(r)$ of the pure hard-sphere fluid at different packing fractions. In (a) the result from this work, Eq. (20), is compared to data from simulations by Groot *et al.* [28] for different packing fractions η. The relative deviations from the result c_{WBII} obtained with the WBII functional [24] are plotted for (b) $\eta = 0.31$ and (c) $\eta = 0.47$. The divergence at $r \to 0$ of the result by Santos [25] and Lutsko [26] is in contradiction with the simulations. The result from this work, Eq. (20), is always within 1% of the WBII result.

which is identical to the Percus-Yevick result from integral equations, and

$$c_{\mathrm{CS}}(r) = c_{\mathrm{PY}}(r) + \frac{\eta^3(4-\eta)}{(1-\eta)^4} + \frac{\eta^2(4-33\eta+2\eta^3)}{6(1-\eta)^4}\frac{r}{\sigma} + \frac{\eta^4(4-\eta)}{2(1-\eta)^4}\left(\frac{r}{\sigma}\right)^3, \tag{20}$$

which is within 1% of the WBII result [24] for all packing fractions (see Fig. 1). Most importantly, by construction of the new functional, the unphysical divergence of $c(r)$ for $r \to 0$, which occurs in the original proposal by Santos [25,26], is no longer observed (see Fig. 1). The new expression $c_{\mathrm{CS}}(r)$ from Eq. (20), like the WBII result, describes the simulation data of Groot *et al.* [28] very well for low packing fractions. Deviations start to occur around $\eta = 0.3$, becoming more pronounced as η is increased further. However, deviations are always less than 5%, which has to be compared to the PY results for the direct correlation function, which deviates from the simulations by more than 10%.

In order to keep the resulting functional simple as to allow for efficient numerical computations, we restrict ourselves to $m \leqslant 2$ in the present work. In the following we investigate two alternative routes that allow us to determine the remaining coefficient function f_2.

A. Functionals based on dimensional crossover

Considering that Φ_m becomes exact in the strict 0D limit and that it is based on a given EOS in the homogeneous 3D fluid system, it appears natural to determine f_2 such that homogeneous systems of intermediate dimensions are also accurately described. We focus on the 1D homogeneous limit of Φ_m for which the free energy is known exactly. It turns out that f_2 can be chosen such that the functional yields the exact free energy of the homogeneous 1D system (see Appendix B). We find that

$$\begin{aligned} f_2(y) = {} & \tfrac{1}{8}(35+78y+54y^2)f_0(y) \\ & + \tfrac{1}{8}(13+18y)(1+3y)yf_0'(y) \\ & + \tfrac{1}{8}(1+3y)^2y^2f_0''(y) - \tfrac{1}{4}(7+6y)f_1(y) \\ & - \tfrac{1}{4}(1+3y)yf_1'(y), \end{aligned} \tag{21}$$

which for the respective EOSs reads

$$\begin{aligned} f_2^{\mathrm{PY}}(y) &= \frac{3}{8}(7+22y+18y^2) \\ f_2^{\mathrm{CS}}(y) &= \frac{15+69y+221y^2+438y^3+459y^4+246y^5+54y^6}{12y(1+y)^3} \\ &\quad - \frac{5\ln(1+y)}{4y^2} \\ &= \frac{3}{8}\left(7+22y+\frac{19}{2}y^2\right) + \mathcal{O}(y^3). \end{aligned} \tag{22}$$

We test the functional by applying it to a homogeneous fluid of hard disks in 2D. The calculation is analogous to the dimensional reduction performed by Rosenfeld *et al.* (see Appendix A of Ref. [18]). In Fig. 2 we compare the pressure resulting from the different functionals (PY/CS, $m = 1,2$) to the accurate hard-disk EOS given by Solana and coworkers [29]:

$$\frac{\beta p_{\mathrm{MCS}}}{\rho} = \frac{1+\eta^2/8-\eta^4/10}{(1-\eta)^2}. \tag{23}$$

We also include the pressure obtained upon dimensional reduction of Rosenfeld's original FMT [17] and the more recent White Bear II version of FMT [24].

Clearly, Fig. 2 shows that the functional Φ_2^{CS} yields the best result for the pressure upon dimensional reduction to the homogeneous 2D hard-disk fluid with a deviation from

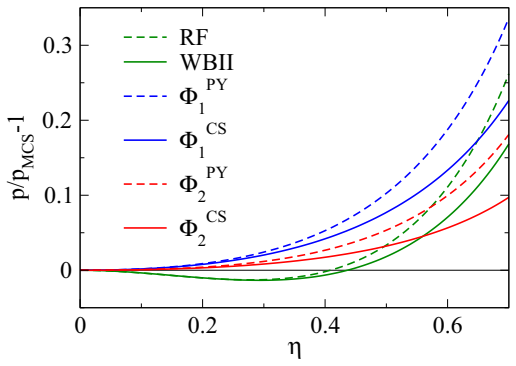

FIG. 2. (Color online) Pressure of the homogeneous hard-disk fluid in 2D as obtained via dimensional reduction of various functionals (see text for details) compared to the accurate pressure p_{MCS} due to Solana and coworkers [29].

the accurate MCS result, which is always less than 10%. This confirms the expectation that indeed the functional with the best performance for the homogenous 3D system (via the accurate CS EOS) and for the homogeneous 1D system [exact free energy due to f_2^{CS} from Eq. (22)] is also the most accurate in the intermediate case, namely the homogeneous 2D system. The second best result follows from the WBII functional [24] with a maximum deviation of less than 17% while the other functionals give rise to larger deviations between 18% and 34% at the largest 2D packing fraction.

B. Functionals using an empirical parameter

It turns out that the functionals $\Phi_2^{\mathrm{PY/CS}}$ with $f_2^{\mathrm{PY/CS}}$ from Eq. (22) are unsuited for the application to hard-sphere crystals. This can be understood by realizing that even though y vanishes in the strict 0D limit, it can become very large for more general density profiles that involve sharp peaks. For instance in a configuration of two narrow cavities at a distance $d \approx 2R$ a divergence occurs at the contact point of the δ shells (see Appendix A). Hence the fact that for large y we have $f_2 \propto y^2$ makes the resulting functional diverge for crystals. This behavior is not entirely unexpected, considering that the *homogeneous* 1D system for which $f_2^{\mathrm{PY/CS}}$ from Eq. (22) is designed differs a great deal from a crystalline configuration. In the following, we therefore introduce a simple alternative choice of f_2, which does not produce divergences for peaked density distributions.

The alternative that we suggest consists in choosing $f_0^{\mathrm{PY/CS}}$ and $f_1^{\mathrm{PY/CS}}$ as above while simply setting f_2 to a constant λ. We denote the resulting free-energy density by $\Phi_{2,\lambda}^{\mathrm{PY/CS}}$. A free minimization (see Ref. [27] for a description of the corresponding numerical methods) of the resulting functional shows that the expressions $\Phi_{2,\lambda}^{\mathrm{PY/CS}}$ give indeed rise to a hard-sphere crystal phase. In particular, we can study parameters such as the liquid and crystal packing fractions η_{li} and η_{cr}, free energies per particle $(\beta F/N)_{\mathrm{li}}$ and $(\beta F/N)_{\mathrm{cr}}$, as well as the chemical potential $\beta\mu_{\mathrm{coex}}$ at the point of phase coexistence (see Table I). While neither of the functionals $\Phi_{2,\lambda}^{\mathrm{PY/CS}}$ agrees as well with simulation data [30] as the tensorial WBII functional [24,27], the functionals $\Phi_{2,\lambda=0}^{\mathrm{PY}}$ and $\Phi_{2,\lambda=\frac{1}{2}}^{\mathrm{CS}}$ exhibit reasonable agreement with the simulations. In terms of computational

TABLE I. Properties of the coexistence point of the liquid and crystal phases in the pure hard-sphere system as obtained from a free minimization of the various functionals $\Phi_{2,\lambda}^{\mathrm{PY/CS}}$ (see text) and the tensorial WBII functional [24,27] compared to results from simulations [30]. Note that simulation values of $(\beta F/N)_{\mathrm{li}}$, $(\beta F/N)_{\mathrm{cr}}$, and $\beta\mu_{\mathrm{coex}}$ have been obtained by using η_{li} and η_{cr} from Ref. [30] in the appropriate equations of state (see Ref. [15] for details).

	$\Phi_{2,\lambda=0}^{\mathrm{PY}}$	$\Phi_{2,\lambda=\frac{1}{2}}^{\mathrm{PY}}$	$\Phi_{2,\lambda=1}^{\mathrm{PY}}$	$\Phi_{2,\lambda=0}^{\mathrm{CS}}$	$\Phi_{2,\lambda=\frac{1}{2}}^{\mathrm{CS}}$	$\Phi_{2,\lambda=1}^{\mathrm{CS}}$	WBII	SIM
η_{li}	0.484	0.475	0.467	0.513	0.503	0.490	0.495	0.492
η_{cr}	0.521	0.509	0.505	0.555	0.536	0.525	0.544	0.545
$(\beta F/N)_{\mathrm{li}}$	3.45	3.17	2.95	4.21	3.86	3.47	3.82	3.75
$(\beta F/N)_{\mathrm{cr}}$	4.58	4.16	3.98	5.68	4.98	4.52	4.96	4.96
$\beta\mu_{\mathrm{coex}}$	16.24	15.07	14.08	18.43	17.29	15.89	16.38	16.09

complexity the latter functionals are advantageous as they do not make use of a tensorial weighted density.

Another rigorous test of a density functional is the computation of the (relative) vacancy concentration n_{vac} of the hard-sphere crystal in equilibrium (defined as the ratio of the number of vacant lattice sites to the total number of lattice sites). In order to obtain the equilibrium vacancy concentration, the free energy per particle must be minimized (at fixed bulk density) with respect to the density distribution in the face-centered cubic (fcc) unit cell as well as the side length of the unit cell, and the presence of vacancies is manifest by an average occupation of the fcc unit cell of less than 4. At present, only FMT-type functionals can deliver values for n_{vac}, which are of the correct order of magnitude ($\sim 10^{-4}$, see Ref. [31] for a theoretical explanation of this order of magnitude). Other functionals (such as Taylor expanded functionals or the PFC model) give $|n_{\mathrm{vac}}| \sim O(0.1)$, with even possibly negative signs (corresponding to a presence of excess interstitials which is unphysical for the hard sphere system) [15]. Crucial for the correct order of magnitude of n_{vac} is

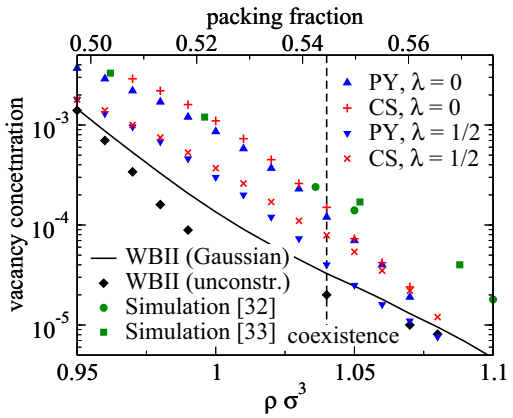

FIG. 3. (Color online) Vacancy concentration n_{vac} of the hard-sphere crystal as a function of the packing fraction η. The results for the functionals $\Phi_{2,\lambda=0}^{\mathrm{PY/CS}}$ and $\Phi_{2,\lambda=\frac{1}{2}}^{\mathrm{PY/CS}}$ were obtained using unconstrained minimization of the functional while results for the tensorial WBII functional were obtained using both unconstrained and Gaussian minimization [27]. For comparison, we show simulation results from Kwak *et al.* [32] as well as from Bennett and Alder [33].

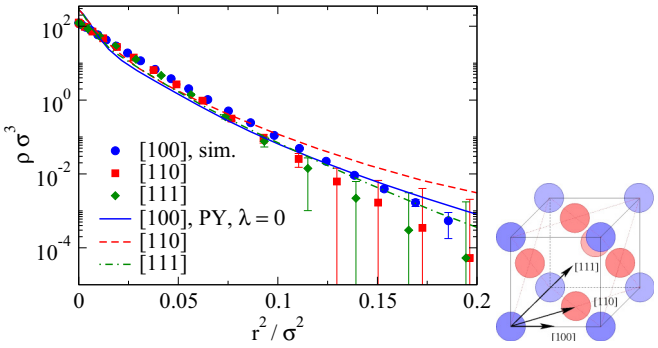

FIG. 4. (Color online) Sections through the density distribution around fcc lattice sites along the lattice directions [100], [110], and [111] for the bulk density $\rho\sigma^3 = 1.04$. The x axis denotes the squared distance from the lattice site and the y axis corresponds to the logarithmic density such that a Gaussian distribution would be a straight line. Full symbols with error bars are Monte Carlo simulation data from Ref. [27] and the lines are results from $\Phi^{\mathrm{PY}}_{2,\lambda=0}$. The cartoon indicates the lattice directions in the standard fcc unit cell.

the correct 0D-limit of the functionals [27], which is not respected at all by the other approximations. The ability to find a stable crystal with a well-defined value of n_{vac} as a free energy minimum is essential for further applications as it guarantees that the free interface between the liquid and the crystal phase can be computed from the DFT [15]. Previous work has shown that of the tensorial versions of FMT only the WBII functional does give rise to a well-defined vacancy concentration [27]. Interestingly, both the functionals $\Phi^{\mathrm{PY}}_{2,\lambda}$ and $\Phi^{\mathrm{CS}}_{2,\lambda}$ give a stable crystal with vacancy concentrations n_{vac} that compare reasonably well with simulations [32,33], provided that the value of λ is not too large (see Fig. 3). For $\lambda = 1$, no stable crystal at a finite vacancy concentration is obtained. Note that the agreement of the vacancy concentrations derived from the new functionals $\Phi^{\mathrm{PY/CS}}_{2,\lambda}$ with the simulations is even better than that of the tensorial WBII functional. Giving an example: at solid-liquid coexistence ($\eta \approx 0.545$) n_{vac} is approximately 2×10^{-4} (simulation), 1.2×10^{-4} (PY, $\lambda = 0$), 0.8×10^{-4} (CS, $\lambda = \frac{1}{2}$), and 0.2×10^{-4} (tensorial WBII).

We also investigated the density distributions in the hard-sphere crystal. From simulations, it is known that the distribution is only weakly anisotropic and can be well approximated by a Gaussian function; see Fig. 4 (symbols). The tensorial WBII functional shows a density distribution in very good agreement with the simulation results [27]. The class of functionals investigated here shows a somewhat more pronounced anisotropy in the [110] direction and stronger deviations from a Gaussian [see Fig. 4 (lines) for the example $\Phi^{\mathrm{PY}}_{2,\lambda=0}$]. Close to the lattice site the density distribution is more strongly peaked. The deviations from isotropy and Gaussian shape become stronger with increasing λ, indicating that the approximation $f_2 = \lambda$ should be refined for an accurate description of the full density distribution.

IV. CONCLUSION

Based on Santos' consistent free energy for the uniform hard-sphere mixture we have derived a density functional $\mathcal{F} = \beta^{-1} \int \Phi \, d\mathbf{r}$ in the spirit of Rosenfeld's fundamental measure theory, which has the following properties: The excess free energy density Φ is a solution of the scaled-particle differential equation, Eq. (2), using the weighted densities n_3, n_2, n_1, and n_0 augmented by suitable variables $\bar{n}_2$ and $\bar{n}_1$ that are specific to inhomogeneous systems, Eq. (11). When applied to the bulk fluid, the functional $\mathcal{F}$ reduces to Santos' free energy [25]. Moreover, the direct correlation function $c(r)$ obtained from $\mathcal{F}$ compares well with the previous WBII result and simulation data. In particular, $c(r)$ remains regular for $r \to 0$ unlike the previous result by Santos and Lutsko [25,26]; see Fig. 1. Higher-order terms in $\mathcal{F}$ (f_2 etc.) can be used to make the functional compatible with dimensional reduction; see Fig. 2 for the pressure in a 2D system of hard discs obtained from spatial confinement of the 3D functional. Alternatively, f_2 can be chosen such that the functional $\mathcal{F}$ is suited to describe a hard-sphere crystal, which implies a reasonable characterization of the transition point between the fluid and crystal phases as well as accurate values for the vacancy density of the crystal; see Fig. 3.

The latter point is particularly appealing, considering that so far only the tensorial version of the WBII functional had been shown to give well-defined vacancy densities. Unlike the former, the FMT introduced in the present work only employs scalar and vectorial weighted densities, which makes it computationally more amenable than the tensorial functionals.

Several interesting routes remain open for the future development of FMTs based on Santos' consistent free energy. First of all, a benefit of our theory is that it can be systematically extended. Here we use only the functions f_0, f_1, and f_2 in order to build our functionals while higher orders might be explored in order to potentially reconcile the two avenues of construction employed in this work. This is dimensional reduction on the one hand (see Sec. III A) and avoidance of divergences for peaked density distributions on the other (see Sec. III B). Higher-order terms f_k, with $k > 2$, might allow one to construct a functional that reduces correctly also for some *inhomogeneous* 1D density distributions while not being plagued by divergences that prohibit it from being used for the crystal. However, this approach would most likely require some rather lengthy algebra so that in view of the powerful tensorial WBII functional it is not clear if the effort is actually worthwhile.

Finally, we emphasize that, while the general solution of the augmented scaled-particle equation, see Φ_{gen} in Eq. (12), does apply to mixtures, we were forced to reduce the functional to the one-component system for most of this work in order to be able to specify the remaining degrees of freedom in Eq. (12), i.e., the unknown function F therein. There is surely a lot of territory to be explored in the direction of deriving a mixture FMT based on Santos' free energy. Exact results for the virial coefficients of binary mixtures [34,35] might serve as a starting point. We conclude that the FMT functional introduced in this work, which is based on the most general solution of the augmented scaled-particle differential equation, is likely to provide the foundation for many further developments.

APPENDIX A: 0D LIMIT

In the strict 0D limit the density distribution is given by $\rho(\mathbf{r}) = \eta\delta(\mathbf{r})$, where $0 \leqslant \eta \leqslant 1$ is the 0D packing fraction and r is the distance from the origin, where the density is concentrated. The weighted densities n_3, n_2, and $\mathbf{n}_2$ are readily calculated from Eqs. (7) and (8) to be $n_3(r) = \eta\Theta(R-r)$, $n_2(r) = \eta\delta(R-r)$, and $\mathbf{n}_2(\mathbf{r}) = \eta\delta(R-r)\hat{\mathbf{r}}$. Hence, from Eq. (11) we have $\bar{n}_2 \equiv 0$. Noting that for a fluid of spheres of only one size the weighted density $\bar{n}_1$ is equal to $\bar{n}_2$ up to a constant factor we find that both $\bar{n}_1$ and $y = \frac{R\bar{n}_2}{3(1-n_3)}$ also vanish in the strict 0D limit. Given the fact that F in Eq. (12) is finite for $y \to 0$ it follows that in the strict 0D limit only the first term $-n_0 \ln(1-n_3)$ of Φ_{gen} contributes, which is indeed known to yield the exact free energy of a 0D cavity [18].

Consider now a situation where two 0D cavities with packing fractions η_1 and η_2 are at a distance $d \approx 2R$. It can be shown that the first two terms of Φ_{gen} from Eq. (12) yield the exact free energy. However, unlike in the case of just one isolated 0D cavity considered above, the third term of Φ_{gen} does generally not vanish. This can be seen by examining the leading order behavior of the weighted densities at the contact point of the δ shells, i.e., midway between the two cavities. Denoting the width of the δ shells by Δ, we have $n_2 \propto (\eta_1+\eta_2)\Delta^{-1}$ and $\mathbf{n}_2 \propto (\eta_1-\eta_2)\Delta^{-1}\hat{\mathbf{r}}$, where the difference of the packing fractions is a result of the opposing orientations of the vectors entering the calculation of $\mathbf{n}_2$. From this we find that $\bar{n}_2 \propto \frac{4\eta_1\eta_2}{\eta_1+\eta_2}\Delta^{-1}$. As a result, $\bar{n}_2$ and therefore y no longer vanish in the case of *two* 0D cavities that are in proximity. The dependence on the inverse of the cavity size shows that y can in fact assume large values when evaluated for peaked density distributions such as they occur for the hard-sphere crystal. The limit of large y can be easily worked out for the present functionals. Since $f_0^{\text{PY}} = 1$ and $f_1^{\text{PY}} = 1$ the third term of the PY functional reads $\bar{n}_2^3/24\pi(1-n_3)^2$, which has been shown to remain finite when integrated over configurations of hard-sphere crystals [18]. Interestingly, for large y we find $f_0^{\text{CS}} \to \frac{2}{3}$ and $f_1^{\text{CS}} \to \frac{2}{3}$. Again, the values coincide and we can borrow the arguments from the PY functional to show that also the CS functional is suited for the hard-sphere crystal. The picture changes as we include $f_2^{\text{PY/CS}}$ from Eq. (22). For large y we have $f_2^{\text{PY/CS}} \propto y^2$, which, as it turns out, makes the resulting functional unstable when applied to hard-sphere crystals. Choosing f_2 as a constant, however, allows us to properly treat crystalline density distributions.

APPENDIX B: 1D HOMOGENEOUS FLUID

We consider a homogeneous hard-sphere fluid in 1D with number density ρ (in units of 1/length). We choose cylinder coordinates (r, φ, z) such that the fluid is located along the z axis. The weighted density n_3 is readily calculated to be $n_3(r) = 2\rho\sqrt{R^2-r^2}\,\Theta(R-r)$, where R is the hard-sphere radius. The remaining weighted densities are obtained using that $n_2(r) = \frac{\partial}{\partial R}n_3(r)$ and $\mathbf{n}_2(\mathbf{r}) = -\frac{\partial}{\partial r}n_3(r)\mathbf{e}_r$. One finds that $n_2(r) = \frac{2\rho R}{\sqrt{R^2-r^2}}\Theta(R-r)$ and $\mathbf{n}_2(\mathbf{r}) = \frac{2\rho r}{\sqrt{R^2-r^2}}\Theta(R-r)\mathbf{e}_r$. It follows from Eq. (11) that $\bar{n}_2(r) = \frac{2\rho}{R}\sqrt{R^2-r^2}\Theta(R-r)$ and hence $x = \frac{\bar{n}_2}{n_2} = 1 - \frac{r^2}{R^2}\Theta(R-r)$. We now make use of the fact that the first two terms of Φ_m from Eq. (13), namely $\frac{-n_2\ln(1-n_3)}{4\pi R^2} + \frac{\bar{n}_2 n_2}{4\pi R(1-n_3)}$, yield the *exact* free energy of the homogeneous 1D fluid. In fact, it can be shown that the two terms yield the exact density functional even in the inhomogeneous case. Consequently, in order to obtain the exact free energy for the homogeneous 1D fluid we must require the third term in Eq. (13) to vanish in the homogeneous limit. Using the above expressions for the weighted densities and setting R to unity this translates to the condition that

$$\int_0^1 r\,y\,(1+3y)\left[f_0(y) - \sum_{k=1}^{m} f_k(y) r^{2k}\right] dr \stackrel{!}{=} 0, \tag{B1}$$

where $y = \frac{\eta\sqrt{1-r^2}}{3(1-\eta\sqrt{1-r^2})}$ with the 1D packing fraction $\eta = 2R\rho$. In the following we consider only the case where $m = 2$. Changing the integration variable from r to y and multiplying with a constant leads to

$$\int_0^{\frac{\eta}{3(1-\eta)}} u^2\{\eta^4 f_0(y) - \eta^2 f_1(y)(\eta^2-u^2) - f_2(y)(\eta^2-u^2)^2\} \times dy \stackrel{!}{=} 0, \tag{B2}$$

where $u = \frac{3y}{1+3y}$.

The condition expressed in Eq. (B2) is equivalent to requiring that the left-hand side of Eq. (B2) at $\eta = 0$ and all derivatives with respect to η at $\eta = 0$ vanish. Since the integrand is a quartic polynomial in η differentiating Eq. (B2) five times with respect to η makes the integral disappear and a second-order linear differential equation for f_2 is obtained, which can be solved to yield Eq. (21). Integration constants are determined from the condition that f_2 has to be finite for $y \to 0$. The result can be cross-checked by inserting it into Eq. (B2) and eliminating derivatives of f_0 and f_1 using integration by parts.

[1] P. N. Pusey and W. van Mengen, Nature **320**, 340 (1986).
[2] S. Sokolowski and J. Fischer, Mol. Phys. **68**, 647 (1989).
[3] J. D. Weeks, D. Chandler, and H. C. Andersen, J. Chem. Phys. **54**, 5237 (1971).
[4] W. G. Hoover and F. H. Ree, J. Chem. Phys. **49**, 3609 (1968).
[5] Edited by A. Mulero, *Theory and Simulation of Hard-Sphere Fluids and Related Systems*, Lect. Notes Phys. 753 (Springer, Berlin/Heidelberg, 2008).
[6] J. K. Percus and G. J. Yevick, Phys. Rev. **110**, 1 (1958).
[7] J. L. Lebowitz, Phys. Rev. **133**, A895 (1964).
[8] R. Kjellander and S. Sarman, Chem. Phys. Lett. **149**, 102 (1988).
[9] J. M. Brader, J. Chem. Phys. **128**, 104503 (2008).
[10] S. Lang, V. Botan, M. Oettel, D. Hajnal, T. Franosch, and R. Schilling, Phys. Rev. Lett. **105**, 125701 (2010).
[11] A. Jaiswal, A. S. Bharadwaj, and Y. Singh, J. Chem. Phys. **140**, 211103 (2014).

[12] R. Evans, in *Fundamentals of Inhomogeneous Fluids*, edited by D. Henderson (Dekker, New York, 1992).
[13] R. Roth, J. Phys.: Condens. Matter **22**, 063102 (2010).
[14] H. Emmerich, H. Löwen, R. Wittkowski, T. Gruhn, G. I. Toth, G. Tegze, and L. Granasy, Adv. Phys. **61**, 665 (2012).
[15] M. Oettel, S. Dorosz, M. Berghoff, B. Nestler, and T. Schilling, Phys. Rev. E **86**, 021404 (2012).
[16] R. Evans, Adv. Phys. **28**, 143 (1979).
[17] Y. Rosenfeld, Phys. Rev. Lett. **63**, 980 (1989).
[18] Y. Rosenfeld, M. Schmidt, H. Löwen, and P. Tarazona, Phys. Rev. E **55**, 4245 (1997).
[19] P. Tarazona and Y. Rosenfeld, Phys. Rev. E **55**, R4873 (1997).
[20] P. Tarazona, Phys. Rev. Lett. **84**, 694 (2000).
[21] N. F. Carnahan and K. E. Starling, J. Chem. Phys. **51**, 635 (1969).
[22] R. Roth, R. Evans, A. Lang, and G. Kahl, J. Phys. Condens. Matter **14**, 12063 (2002).
[23] Y. X. Yu and J. Wu, J. Chem. Phys. **117**, 10156 (2002).
[24] H. Hansen-Goos and R. Roth, J. Phys.: Condens. Matter **18**, 8413 (2006).
[25] A. Santos, Phys. Rev. E **86**, 040102(R) (2012).
[26] J. F. Lutsko, Phys. Rev. E **87**, 014103 (2013).
[27] M. Oettel, S. Görig, A. Härtel, H. Löwen, M. Radu, and T. Schilling, Phys. Rev. E **82**, 051404 (2010).
[28] R. D. Groot, J. P. van der Eerden, and N. M. Faber, J. Chem. Phys. **87**, 2263 (1987).
[29] A. Mulero, I. Cachadiña, and J. R. Solana, Mol. Phys. **107**, 1457 (2009).
[30] T. Zykova-Timan, J. Horbach, and K. Binder, J. Chem. Phys. **133**, 014705 (2010).
[31] M. Mortazavifar and M. Oettel, Europhys. Lett. **105**, 56005 (2014).
[32] S. K. Kwak, Y. Cahyana, and J. K. Singh, J. Chem. Phys. **128**, 134514 (2008).
[33] C. H. Bennett and B. J. Alder, J. Chem. Phys. **54**, 4796 (1971).
[34] S. Labík and J. Kolafa, Phys. Rev. E **80**, 051122 (2009); **84**, 069901(E) (2011).
[35] I. Urrutia, Phys. Rev. E **84**, 062101 (2011).